

Structure – Directing Effect of Renewable Resource Based Amphiphilic Dopants on the Formation of Conducting Polyaniline-Clay Nanocomposite

Janardhanannair D. Sudha,* Viswan L. Reena

Summary: The structure-directing effect of two amphiphilic dopants on the nucleation and growth mechanism during the formation of micro/ nanostructured polyaniline (PANI) and polyaniline-clay nanocomposites (PANICNs) is described. PANIs and PANICNs were prepared by in-situ intercalative emulsion polymerization of aniline using the amphiphilic dopants, 3-pentadecyl phenyl phosphoric acid (3-PDPPA) and 3-pentadecyl phenol-4-sulphonic acid (3-PDPSA), derived from cashew nut shell liquid, a renewable resource. These molecules act as intercalating agents, dopants and also as structure-directing agents. X- ray diffraction (XRD) and scanning electron microscopic (SEM) studies revealed the formation of lamellar/fibrillar – network in PANI- PDPPA and cylinder/rod morphology in PANI-PDPSA. Experimental data reveal that fibrillar morphology arises from the heterogeneous nucleation followed by an indefinite growth mechanism. On the other hand rod-like structures are formed from the self-assembled rod-like micelle guided polymerization through homonucleation followed by an anisotropic growth mechanism. Electrical conductivity measurement revealed lower conductivities for PANICNs than that of PANIs.

Keywords: clay; conducting; dopant; micelle; nanocomposite; polyaniline; structure-directing agent

Introduction

In recent years, electrically conducting polymer-clay nanocomposite comprising of nanofibers and nanotubes have been prepared by different strategies for potential applications as chemical sensors, actuators, light emitting diodes and gas separation membranes.^[1–3] Conjugated polymers encapsulated in two-dimensional layers of inorganic hosts offer fascinating strategies for designing materials with intriguing properties. The constrained environment of an inorganic host should lead to a high degree of polymer order within the host, and this may have profound effects on polymer

structure, properties, and electrical conduction mechanisms. These systems represent a new class of molecular composites with diverse electrical, optical, mechanical, and thermal properties. Polyaniline (PANI) being one of the versatile conducting polymer has received attention for the preparation of conducting polymer-clay nanocomposites.^[4] Generally PANI nanofibers and nanotubes have been prepared by chemical or electrochemical oxidation polymerization of aniline with the aid of either templates or structure-directing molecules.^[5,6] Literature reveals that the hydrophobic moiety of the structure-directing agent is able to direct the formation of PANI micro/nanotubes from anionic surfactant micelles.^[7] Mesomorphic behavior of self-assembled complexes of methyl sulphonic acid (MSA), polyvinyl pyridine (PVP) and 3-PDP(3- pentadecyl phenol), which is the starting material for

Chemical Sciences and Technology Division, National Institute for Interdisciplinary Science and Technology (NIST), CSIR, Thiruvananthapuram 695019, India
Fax: 0091-471-2491712
E-mail: sudhajd2001@yahoo.co.in

the preparation of PDPSA, and PDPPA was reported by Ikkala et al.^[8]

There are number of reports on the preparation and properties of lamellar nanocomposites of polyaniline with various layered materials.^[9] Bentonite clay is one of the most abundant naturally occurring layered materials having high aspect ratio and high surface area. In addition, the surface of the bentonite is easily amenable for modification. They contain thin layers of aluminum silicate, organized themselves in a parallel fashion to form stacks with a regular van der Waals gap in between them called interlayer spacing or gallery. In the interlayer region there exists Na^+ and Ca^{2+} , which can be replaced with the alkyl ammonium or alkylphosphonium ions.^[10] One of the commonly used methods to prepare nanocomposites is intercalation of aniline into the gallery of clay layers using dodecylbenzene sulphonic acid (DBSA) as intercalating agent cum dopant followed by in-situ polymerization.^[11] The presence of both hydrophobic and hydrophilic groups present in DBSA enables it to function as a surfactant. This can reduce the inter gallery interaction and maximize the affinity between hydrophilic host (clay) and hydrophobic guest (aniline) and also serve as dopant for PANI. A variety of amphiphilic dopants which belong to the families of sulphonic acids,^[12] and phosphonic acids^[13] as well as phosphoric acid esters are reported^[14] Herein we report the use of new amphiphilic dopants derived from 3-pentadecyl phenol (3-PDP)^[15] which is present in cashew nut shell liquid, a renewable resource and their structure-directing ability for the preparation of polyaniline clay nanocomposites.

Experimental Part

Materials

Aniline monomer (99.5% pure, Ranbaxy Chemicals Ltd, Bombay) was distilled under reduced pressure, ammonium persulphate (APS), methyl alcohol (s.d. fine chem limited, Bombay, India) were used without further purification. Bentonite clay

with cation exchange capacity of 55 meq/100 g and a mean chemical formula of $(\text{Na}, \text{Ca})_{0.33}(\text{Al}_{1.67}\text{Mg}_{0.33})\text{Si}_4\text{O}_{10}(\text{OH})2\text{nH}_2\text{O}$ (Loba Chemie, Bombay, India) was washed by saturated sodium chloride solution many times and size fractionated to obtain Na-bentonite free of impurities. Dodecyl benzene sulphonic acid (DBSA) (85% in isopropanol) is obtained from Aldrich. 3-pentadecyl phenyl phosphoric acid (PDPPA)^[3] and 3-pentadecyl phenol-4-sulphonic acid (PDPSA)^[12b] were prepared from 3-pentadecyl phenol (cardanol) which is obtained by the double distillation of cashew nut shell liquid (cashew export promotion council, India) at 3–4 mm Hg at 230–235 °C.

Preparation of PANIs and PANICNs

A general procedure for preparing PANIs and PANICNs is as follows. PANICNs were prepared by the *in situ* intercalative emulsion polymerization method as reported earlier.^[9] 2.5 g of bentonite was taken in a three-necked flask fitted with a mechanical stirrer and reflux condenser. Then dispersed in 200 ml of deionised water by heating and stirring at 80 °C for 3 h. An aqueous solution of aniline 2.5 g (0.029 moles) containing 11.04 g (0.029 moles) of 3-PDPSA was then added drop wise to the clay dispersion. Heating and stirring continued for 2–6 h. The mixture was cooled down to 0 °C by keeping in an ice bath and a solution of APS (0.03 mole) dissolved in 50 ml water was added drop wise to initiate the polymerization. Reaction was continued for 3–4 h. PANICN was isolated by precipitating from methanol. It was then filtered, washed with deionised water, finally with methanol and then dried in a vacuum oven for 2 days at 60 °C. Similar procedures were adopted for the preparation of PANICNs using 3-PDPPA, and DBSA. PANI-PDPSA, PANI-PDPPA and PANI-DBSA were prepared without clay for comparison.

Measurements

UV-vis absorption spectra were recorded using UV-vis spectrophotometer [Shimadzu

model 2100]. FT-IR spectra were recorded on Nicolet impact 400D FT-IR spectrophotometer. X-ray diffraction were obtained on a Philips X'pert Pro X-ray diffractometer. Electrical conductivity (σ_{dc}) of uniform sized pressed pellets was measured using four probe method using Scientific Equipment, Roorkee (India). Morphological studies of PANICNs pelletised powder samples were studied using scanning electron microscope (SEM, JEOL make, model JSM 5600 LV) at 15 kV accelerating voltage.

Results and Discussion

Synthesis of PANIs and PANICNs

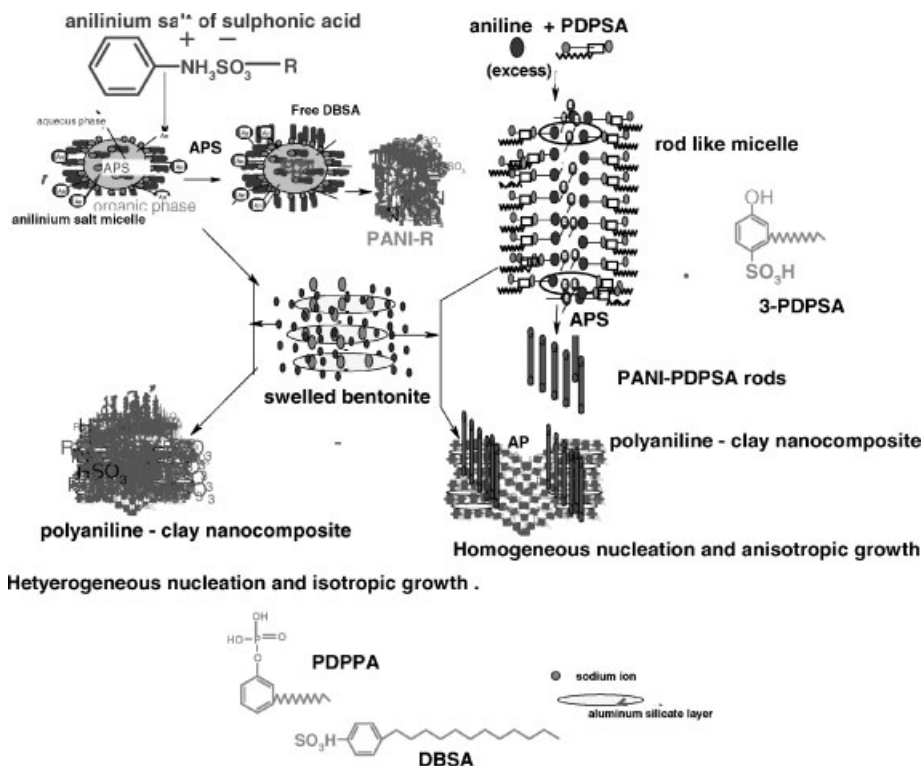
PANICNs were prepared by the *in situ* intercalative emulsion polymerization of anilinium salt complexes of the amphiphilic acids in aqueous dispersion of bentonite using APS as oxidant initiator as shown in scheme.^[3] After the insertion of An^+ into the galleries, a coordinate bond is formed between the monomer and the ions present in the silicate gallery. When the chain adds to a new monomer, it is reduced and reoxidised through the medium. The polymer chain can add monomer until its oxidation stage achieves emeraldine green form and then polymerization stops.

The micro/nano structured fibers or ribbons for PANI-PDPPA and PANI-DBSA observed during the microscopic observation can be suggested through heterogeneous nucleation followed by isotropic growth mechanism as shown in scheme. When aniline is mixed with amphiphilic sulphonic acid, PDPPA⁺⁻A salt is formed by an acid-base reaction. The aniline salt forms self assembled micelles through electrostatic layer by layer assembling. Polymerization starts with the formation of nucleation centres which increases as the reaction proceeds. Once the density of nucleation centers becomes high, the interfacial energy between them may be minimized^[16] and rapid precipitation occurs in a disordered manner yielding irregular fibrillar shaped protonated PANIs

(Scheme 1). The formations of nano/microstructured ribbons/fibers were confirmed by SEM observation and are described in the morphology section.

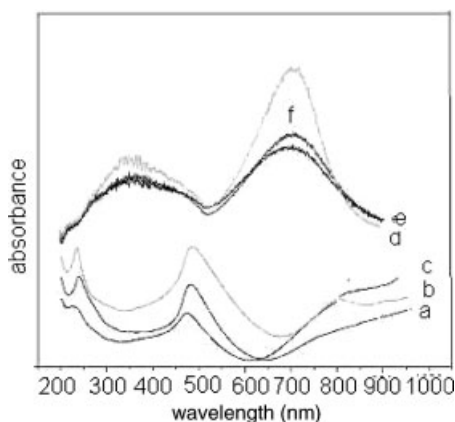
The micro/nano-rods or cylinders observed for PANI-PDPSA and PANICN-PDPSA are possible through “rod like micelle” guided template polymerization as shown in scheme. PDPSA contains two hydrophilic groups (SO_3^- and OH) on the aromatic ring along with long alkyl chain in the meta position of OH group and para to the $-SO_3H$. The amphiphilic nature of An^+PDPSA^- salt facilitate the formation of rod-like micelles and provides a wide variety of active sites for nucleation.^[17] The free aniline can diffuse into the center of the micelles to form core. This was aided through stirring of the aniline- PDPSA for 4–5 hrs before APS was added. The diffusion of aniline monomers into the hydrophilic micelle core enables the polymerization in presence of APS. PANI nanoparticles would aggregate on the surface of the micelle through interaction including hydrogen bonding, π - π interactions and ELBLS.^[8] These nucleated nanoparticles (homogeneous nucleation) undergo end-on attachment of the micelles resulting in linear growth of the nanostructure to form nanometer sized cylinders which further aggregate to form micro cylindrical structures both in PANI-PDPSA and PANICN-PDPSA. Similar studies on the interaction of alkyl chain having polar head group of the organic molecule with the clay surface, which form self-assembled structure on the clay surface, was reported by Brindley.^[18]

The chemical and electronic structure of PANIs and PANICNs were studied using FT-IR and UV-vis spectrometries, respectively. UV-vis spectral technique is a very sensitive tool for studying the nature of PANI protonation and show obvious difference between PANIs and PANICNs. The UV-vis spectra of PANICN-PDPSA, PANICN-DBSA, PANICN-PDPPA, PANI-PDPPA, PANI-PDPSA and PANI-DBSA are shown in Figure 1 a-f, respectively. Generally PANIs exhibited two broad

**Scheme 1.**

Synthesis of PANI s and PANICNs.

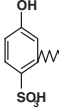
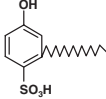
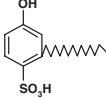
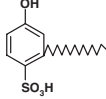
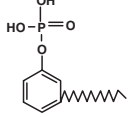
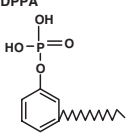
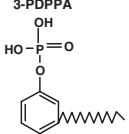
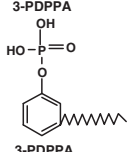




absorption maxima in the range of 340–400 nm and 700–720 nm. The absorption peak in the 340–400 nm can be assigned as the $\pi-\pi^*$ transition in the reduced unit of

**Figure 1.**

UV-vis spectra of PANICN-DBSA (a), PANICN-PDPPA (b), PANICN-PDPSA (c), PANI-DBSA (d), PANICN-PDPPA (e), PANICN-PDPSA (f).

polyaniline.^[19] The strong absorption peak observed at ~ 700 nm is due to the head to tail coupling of anilinium radical cations of the PANI-ES. But in PANICNs, three absorption maxima were observed in the region of 300 nm, 470 nm and 900 nm, respectively. The absorption peak at 470 and 900 nm revealing that PANICNs are in the conducting state (emeraldine salt). The shifting of the two peaks in PANICN to higher wavelength is consistent with the delocalization of electrons in the polaron band promoted by the extended chain conformation of the doped PANI chains inside the nano clay layers.^[20] FT-IR spectra showed that the vibration bands of PANICNs (C=C stretching deformation of the quinoid shifted from 1590 cm^{-1} to 1572 cm^{-1} and that of the benzenoid ring from 1502 to 1485 cm^{-1} in PANIs indicated longer effective conjugation lengths.^[21] However, the C–N stretching vibration in PANICN at 1303 cm^{-1} is slightly higher

Table 1.
Details of the preparation of PANIs and PANICNs.

Sample	Ratio of aniline: opant	Conductivity S/cm	Morphology	XRD d-spacing Å
Bentonite	–	–	Layered texture	12.1
 PANI-PDPSA	1:1	8.2×10^0	Tetrgonal/hexagonal rod like crystallites	28.38, 11.17
 PANICN-PDPSA2	1:1	1.18×10^{-1}	Nano/micro rods	37.92, 18.71
 PANICN-PDPSA3	1:1.5	4.3×10^0	Micro cylinders	45.82, 18.9
 PANICN-PDPSA4	1:2	5.11×10^0	Micro cylinders	46.5 (exfoliated)
 PANI-PDPPA	1:1	8.2×10^{-1}	Layered ribbons	13.6
 PANICN-PDPPA2	1:1	1.28×10^{-3}	Corel fiber like morphology	34,16.7
 PANICN-PDPPA3	1:1.5	8.8×10^{-3}	Nano/micro structured fibri work	42.2, 16.9
 PANICN-PDPPA4	1:2	7.2×10^{-2}	Nano/microstructured ribbons with white spots on the surface	43.(exfoliated)
 PANI-DBSA	1:1	3×10^0	Layerd/ribbon type	28
 PANICN-DBSA2	1:1	8.8×10^{-2}	nano structured fibrillar network	40, 16.7
 PANICN-DBSA3	1:1.5	2.20×10^{-1}	Micro/nano structured fibrillar net work	43.1, 16.41
 PANICN-DBSA4	1:1.2	7.1×10^{-1}	Nano structured fibrillar net work	43.6 (exfoliated)

than that of PANIs at 1301 cm^{-1} . This is caused by the hydrogen bonding interaction between PANI and the basal surface of nano clay (i.e. $\text{NH}\cdots\text{O}$ hydrogen bonding).^[22]

X-ray Diffraction (XRD)

XRD is an efficient analytical tool to probe for determining the degree of intercalation/exfoliation of clay and orientation of clay-polymer nanocomposite. During intercalation, the PANI-dopant chains get confined in the clay layers and the distance between the clay layers increases in various ways depending on the structure of intercalating agent, preparation technique, nature of the interlayer cation and layer charge density.^[23] The details of the effect of the amount and the structure of the amphiphilic molecule on the extent of intercalation/exfoliation are illustrated in Table 1. Typical XRD patterns of bentonite, PANI-DBSA, PANICN-DBSA, PANI-PDPPA, PANICN-PDPPA2, PANI-PDPSA and PANICN-PDPSA2 are shown in Figure 2a–g, respectively. The d-spacing

of the nanocomposite was calculated from the $\langle 001 \rangle$ reflection peak of the clay. Bentonite showed diffraction peak at $2\theta = 7.2^\circ$ corresponding to an interlayer spacing of 12.1 \AA (d_{001} spacing). Diffractogram of PANI-DBSA showed reflection with d-spacing 27 \AA corresponding to the lamellar thickness of the self-assembled layered structure of PANI-DBSA as observed by Taka et al.^[24] PANICN-DBSA exhibited two diffraction maxima with d-spacing of 16.4 \AA and 38 \AA . The initial peak observed is due to the enhancement in the interlayer spacing associated with the confinement of the PANI-DBSA chains. The enhancement in the interlayer spacing of 6.8 \AA is calculated by considering the thickness of the anhydrous aluminum silicate framework as 9.6 \AA . This dimension is very close to the dimension of monolayer of protonated polyaniline that is confined in layered materials like V_2O_5 ^[25] and FeOCl .^[26] The second reflection is due to the distorted layered arrangement of the protonated PANI-DBSA engulfed on the nanoclay layers.

Diffractogram of PANI-PDPPA exhibited sharp peak at $2\theta = 3.3^\circ$ with d-spacing of 33 \AA which corresponds to thickness of the aggregates formed by the self assembled protonated PANI-PDPPA. PANICN-PDPPA exhibited two reflections at $2\theta = 5.8^\circ$ and 3.1° with d-spacing of 16.7 \AA and 37 \AA . The initial peak observed is due to the enhancement in the interlayer spacing associated with the confinement of the protonated PANI-PDPPA chains. Second peak observed is due to the layered arrangement of PANI-PDPPA engulfed over the clay surface. However, the diffractogram of PANI-PDPSA exhibited two sharp diffraction peaks with d-spacing of 28.38 \AA and 11.17 \AA corresponding to the self-assembled protonated PANI-PDPSA layers. These results are in analogy to the observation made by other researchers.^[27] The sharper and oriented diffractogram observed for PANI-PDPSA may be attributed due to the hydrogen bond interaction between PANI layers with the hydroxyl group of PDPSA. These results were further strengthened by

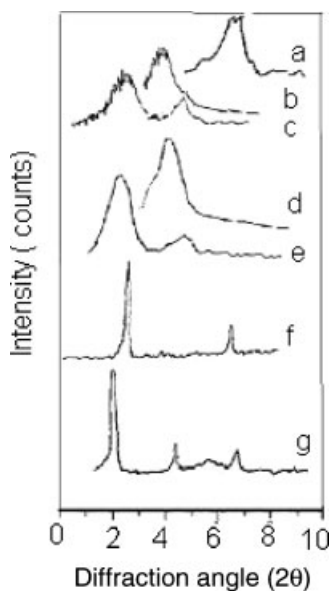


Figure 2.

Bentonite (a), PANI-DBSA (b), PANICN-DBSA (c), PANI-PDPPA (d), PANICN-PDPPA (e), PANI-PDPSA (f), PANICN-PDPSA (g).

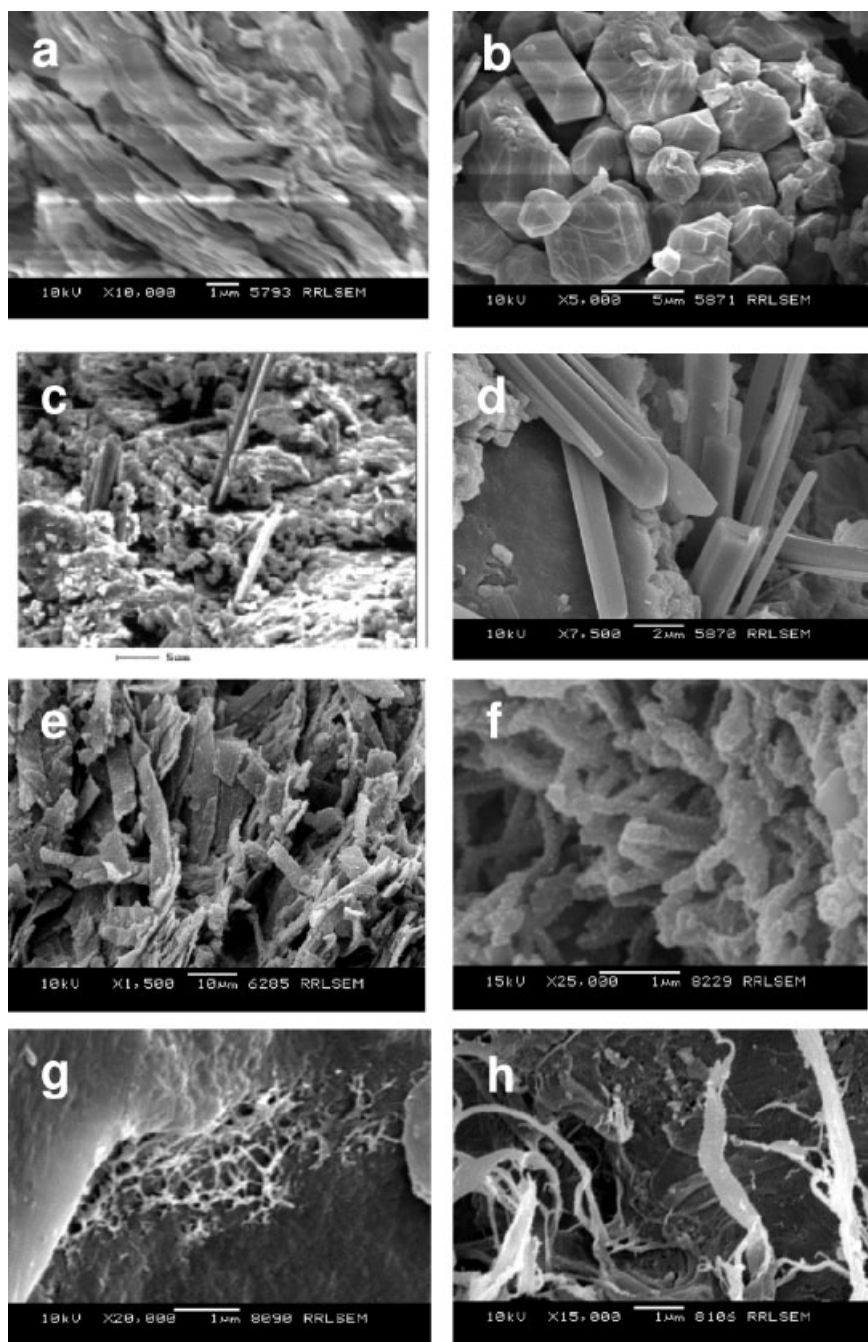


Figure 3.

SEM pictures of (a) PANI-DBSA (layered texture), (b) PANI-PDPSA (hexagonal crystallites), (c) PANICN-PDPSA2 (nano sized rods emerging out of clay layers), (d) PANICN-PDPSA (microstructured cylinders protruding out of clay interlayer), (e) PANI-PDPPA (layered ribbons), (f) core fibril net works with white spots on the surface (g) PANICN (fibrillar net work above the nanoclays) and (h) PANI-DBSA (nano structured ribbons).

the observations made by Ruokolainen et al.^[28] The XRD pattern of PANICN-PDPSA showed sharp peaks with d-spacing of 35.19, 18.58 Å. The enhancement in the interlayer spacing of (d_{001}) ~ 9 Å to the dimension of PANI-PDPSA lying perpendicular to the plane of clay layers. The sharp diffraction peak observed in the lower angle ($2\theta = 1.9^\circ$) with d-spacing of 45 Å corresponds to the thickness of the self-assembled PANI-PDPSA chains engulfed over the nanoclays. The bifunctional PDPSA anion will interact with the PANI chains and hydrated clay layers through hydrogen bonding. Also ionic interaction between the PANI chains and amphiphilic sulphonate anion will induce more orientation and ordering for the former.

It may be interesting to note that the characteristic d_{001} values observed for protonated PANIs vanished in PANICNs and new peaks appeared with a higher d-spacing indicating the formation of the modified layered structures of protonated PANIs as shown in Scheme a and b. This is due to the distortion of the layered arrangement of PANIs by the nano clay layers. At high dopant concentration of 1:2, the characteristic d_{001} peak of bentonite vanished due to the exfoliated structure (random orientation) of the clay layers in the PANICNs. As the ratio of dopant increased from 1:0.5 to 1:2, the inter layer thickness of the self assembled layers of PANIs in PANICN-PDPSA increased from 36–45 Å.

Morphology

The structure-directing effect of the amphiphilic dopants on the morphology of PANI and PANICNs was further studied using SEM. It was observed that the morphology of the PANIs and PANICNs vary with the amount and structure of the amphiphilic dopants. Details of the morphological observation under different conditions are illustrated in Table 1. Typical micrographs of PANIs and PANICNs are shown in figure 3. SEM micrograph of PANI-DBSA (Figure 3a) observed as lamellar shaped layered structures with thickness of 27 Å

(XRD data) and micrograph of PANI-PDPSA (Figure 3b) observed as highly oriented regular hexagonal/tetragonal crystallites with sharp edges. PANI-PDPPA (Figure 3c) observed as layered ribbons of nano/micrometer sized thickness. When the concentration of DBSA increased to 1:2 ratios, long nanometer sized ribbons were observed (Figure 3h). PANICN-PDPSA2 with aniline/dopant ratio 1:1 showed nano sized rods which appeared as originating and growing out of the clay interlayer/surfaces (Figure 3c). When the aniline/PDPSA ratio is increased to 1:2, highly oriented micro structured rods/strips were observed (Figure 3d). These microstructures are formed due to the aggregation of the nanostructured rods.

The micrograph of the PANICN-DBSA exhibited fibrillar network structures engulfed over the nano clay layers (Figure 3 g) due to the heterogeneous nucleation followed by isotropic growth. PANICN-PDPPA showed core shaped fiber morphology. We observed small white spots on the nanofiber surfaces which are associated with asperities along the fibers. We suggest these may act as surface active sites for nucleation. (Figure 3h). These nucleated nanoparticles will form network fibrillar nanostructures through edge to edge collision. The mechanism for the formation of interconnected, branched nanofiber networks observed in PANI-PDPPA, PANICN-PDPPA, PANI-DBSA and PANICN-DBSA is as discussed in the synthesis.

Electrical Conductivity Measurements

The dc conductivity (σ_{dc}) measurements of PANIs and PANICNs were carried out using four-probe conductivity meter with uniform sized pellets. Measurements revealed that electrical conductivity of PANIs and PANICNs showed variation with the amount of dopant and the details are shown in the Table. PANI-PDPPA showed conductivity of 8.2×10^{-1} S/cm (1:1). PANICN-PDPPA exhibited conductivity in the range 1.28×10^{-4} , 1.2×10^{-3} , 8.8×10^{-3} , 7.2×10^{-2} S/cm, when the aniline/PDPPA molar ratio increased from 1:0.5, 1:1, 1:1.5. 1:2

respectively. Conductivity values of PANI-DBSA measured is 3×10^0 S/cm. PANICN-DBSA showed increased conductivity values when the ratio of [aniline]: [DBSA] varied from 1:0.5, 1: 1, 1:1.5, 1:2, and the values were measured to be 3.2×10^{-3} , 8.8×10^{-2} , 2.20×10^{-1} , 7.1×10^{-1} S/cm respectively. Conductivity of PANI-PDPSA is found to be 8.2×10^0 S/cm. PANICN-PDPSA showed conductivity in the order of 7.11×10^{-2} , 1.18×10^{-1} , 4.3×10^0 and 5.11×10^0 S/cm when the [aniline]: [PDPSA] molar ratio varied as 1:0.25, 1:5, 1:1 1:2, respectively. Results revealed that the conductivity is controlled by two factors. The conductivity of PANICNs decreased as the amount of clay is increased, possibly due to the distortion of PANI layered structure by the insulative clay layers. This causes relatively low conductivity in PANICNs compared to PANIs. As the concentration of the dopant increases, the extent of protonation also increases and the number of polarons (radical cations ie charge carriers) increases. During the confinement of the PANI in the insulative clay, it occupies an expanded confirmation and exhibits higher conductivity due to the delocalization of the polaron band with the delocalized electron cloud as observed in UV-vis spectra. These results are in agreement with the observations made by other researchers.^[29]

Conclusions

We have demonstrated the structure-directing effect of renewable resource based amphiphilic dopant for the formation of nano/micro structured cylinders and fibers of polyaniline and showed the utility of self-assembly method for generating such structures. On the basis of the XRD and SEM studies, we suggested the formation of oriented cylinders in PANI-PDPSA which is formed by rod-like micelle guided polymerization by an elongation process through homogeneous nucleation followed by anisotropic growth. In PANI-DBSA,

PANI-PDPPA, the nano/micro ribbons/fibrillar network morphology is formed by a heterogeneous nucleation followed by indefinite growth mechanism. In conclusion, PDPPA and PDPSA derived from renewable resource is a low cost intercalating agent-cum-dopant which can be successfully used as structure directing agent for the preparation of micro/nanostructured polyaniline clay nanocomposite with controlled morphology. The prospects for the direct application of these nanocomposites were found to be easily dispersible with other polymers for making blends for mitigation of electric charge materials and also in electro-optical devices.

Acknowledgements: We are grateful to Indian Space Research Organization for the financial support (GAP 109436). We are also thankful Dr. A. Ajayaghosh, Head, Photosciences and Photonics Group, for valuable discussions.

- [1] [1a] G. M. Nascimento, V. R. I. Constantino, M. L. A. Temperini, *Macromolecules* **2002**, 35, 7535; [1b] J. W. Gilman, C. L. Jackson, A. B. Morgan, R. Hayyis, E. Manias, E. P. Giannelis, M. Wuthenow, D. Hilton, S. H. Phillips, *Chem. Mater.* **2000**, 12, 1866.
- [2] Z. Wei, M. Wan, *Adv. Mater.* **2002**, 14, 1314.
- [3] J. D. Sudha, T. S. Sasikala, *Polymer* **2007**, 48, 338.
- [4] [4a] D. Cardin, *J. Adv. Mater.* **2002**, 5, 553; [4b] M. Thiagarajan, L. A. Samuelson, J. Kumar, A. L. Cholli, *J. Am. Chem. Soc.* **2003**, 125, 11502.
- [5] Z. Wei, M. Wan, *Adv. Mater.* **2002**, 14, 1314.
- [6] B. J. Kim, S. G. Oh, M. G. Han, S. S. Im, *Langmuir* **2000**, 16, 5841.
- [7] [7a] K. Huang, M. X. Wan, *Chem. Mater.* **2002**, 14, 3486; [7b] W. S. Huang, B. D. Humphrey, A. G. MacDiarmid, *J. Chem. Soc., Faraday Trans.* **1986**, 82, 2385; [7c] J. H. Clint, *Surfactant Aggregation*, Blackie, Chapman and Hall, Glasgow, U.K., New York **1991**;
- [7d] H. Xia, H. S. O. Chan, C. Y. Xiao, D. M. Cheng, *Nanotechnology* **2004**, 15, 1807.
- [8] O. Ikkala, G. Ten Brinke, *Chem Commun.* **2004**, 19, 2131.
- [9] [9a] C. R. Martin, *Acc. Chem. Res.* **1995**, 28, 61; [9b] T. A. Kerr, H. Wu, L. F. Nazar, *Chem. Mater.* **1996**, 8, 2005; [9c] T. T. Lan, J. Pinnavaia, *Chem. Mater.* **1994**, 6, 2216.
- [10] R. A. Vaia, R. Krishnamoorthy, *In polymer nanocomposites: Synthesis and Characterization and modeling* Eds: American Chemical Society: Washington DC **2001**, 1.
- [11] B. H. Kim, J. H. Jung, J. W. Kim, H. J. Choi, J. Joo, *Synth. Met.* **2001**, 117, 115.

- [12] [12a] N. Adams, P. Devasagayam, S. J. Pomfret, L. Abell, A. Monkman, *J Phys. Condens. Matter* **1998**, *10*, 8293; [12b] R. K. Paul, C. K. S. Pillai, *Synth. Met.* **2000**, *114*, 27.
- [13] H. S. O. Chan, S. C. Nag, P. K. Ho, *Macromolecules* **1994**, *27*, 2159.
- [14] J. Laska, A. Pron, S. Lefrant, *J Polym Sci A: Polym Chem.* **1995**, *33*, 1437.
- [15] R. K. Paul, Veena Vijayanathan, C. K. S. Pillai, *Synth. Met.* **1999**, *104*, 189.
- [16] [16a] P. A. Hassan, S. N. Sawant, N. C. Bagkar, J. V. Yakhmi, *Langmuir* **2004**, *18*, 2543; [16b] J. Langer, *J Adv. Mater. Opt. Electron* **1999**, *9*, 1; [16c] G. Hous, In: Anionic Surfactant Organic Chemistry, H. W. Stache, J. H. Marcel Clint, Eds., *Surfactant Aggregation*, Blackie, Chapman and Hall, Glasgow, U.K., New York **1991**.
- [17] M. Harada, M. Adachi, *Adv. Mater.* **2000**, *12*, 839.
- [18] G. W. Brindley, W. F. Moll, *The American mineralogist* **1965**, *50*, 1355.
- [19] Y. Cao, P. Smith, A. J. Heeger, *Synth. Met.* **1989**, *32*, 236.
- [20] [20a] J. Yue, A. J. Epstein, *J. Am. Chem. Soc.* **1990**, *112*, 2800; [20b] J. Yue, Z. H. Wang, K. R. Cromack, A. J. Epstein, A. G. Macdiarmid, *J. Am. Chem. Soc.* **1991**, *113*, 2665; [20c] Y. Cao, P. Smith, A. J. Heeger, *Synth. Met.* **1989**, *32*, 263.
- [21] Q. Wu, Z. Xue, Z. Qi, F. Wang, *Polymer* **2000**, *41*, 2029.
- [22] B. H. Kim, J. H. Jung, S. H. Hong, J. S. Joo, A. J. Epstein, K. Mizoguchi, J. W. Kim, H. J. Choi, *Macromolecules* **2002**, *35*, 1419.
- [23] S. A. Chen, G. W. Hwang, *J. Am. Chem. Soc.* **1995**, *117*, 10055.
- [24] T. Taka, J. Laakso, *K Levon. Solid State Commun.* **1994**, *92*, 393.
- [25] C. G. Wu, Y. R. Yeh, J. Y. Chen, Y. H. Chiou, *Polymer* **2001**, *42*, 287.
- [26] [26a] W. Zheng, M. Angelopoulos, A. J. Epstein, A. G. Macdiarmid, *Macromolecules* **1997**, *30*, 2953; [26b] S. A. Chen, G. W. Hwang, *J Am Chem Soc.* **1995**, *117*, 10055.
- [27] [27a] Z. X. Wei, Z. M. Zhang, M. X. Wan, *Langmuir* **2002**, *18*, 917; [27b] J. Langer, *J Adv Mater Opt Electron.* **1999**, *9*, 1.
- [28] R. Rukolainen, T. Makinen, T. Torkkeli, R. Makela, G. Serimaa, G. Ten Brinke, O. Ikkala, *Science* **1998**, *280*, 557.
- [29] V. Mehrotra, E. P. Giannelis, *Solid State Commun.* **1991**, *77*, 1.